

Curzi, M., Cipriani, A., Aldega, L., Billi, A., Carminati, E., Van der Lelij, R., Vignaroli, G., and Viola, G., 2022, Architecture and permeability structure of the Sibillini Mts. Thrust and influence upon recent, extension-related seismicity in the central Apennines (Italy) through fault-valve behavior: *GSA Bulletin*, <https://doi.org/10.1130/B36616.1>.

Supplemental Material

Supplemental Text. Methods

Figure S1. (a) View of the ca. 300 m long tunnel. (b) Entrance of the tunnel, where the NE-verging thrust surface which juxtaposes the Scaglia Bianca limestones onto the Scaglia Rossa limestones (intermediate horses) is exposed. (c) NW-plunging fault-bend fold along the tectonic contact between the structurally highest and the underlying horses (structural site no. 4; see Figs. 2 and 3 for location). The contact is represented by SW-dipping, NE-verging thrusts which juxtapose the Maiolica cherty limestones onto the Marne a Fucoidi marly limestones. (d) Tectonic contact between the structurally highest and the underlying horses (structural site no. 4; see Figs. 2 and 3 for location). The contact is represented by three SW-dipping, NE-verging thrusts which juxtapose the Maiolica cherty limestones onto the Marne a Fucoidi marly limestones. The Maiolica lithotypes form metric lenses characterized by an internal structure imbricated toward NE. The Marne a Fucoidi pelagites exhibit highly (marly) and poorly (calcareous) foliated domains. Note a NW-plunging fault-bend fold above the lower thrust. (e, f) Detail of the metric lensoidal lithons of Maiolica characterized by an internal structure imbricated toward NE and embedded within highly-foliated Marne a Fucoidi pelagites. (g) Highly-foliated Marne a Fucoidi pelagites. (h) Metric imbricated sigmoidal lithons of Maiolica limestones characterized by an internal structure imbricated toward NE.

Figure S2. X-ray diffraction patterns for randomly oriented mounts for the different grain-size fractions of sample GI12 with reflections of illite polytypes.

Table S1. Summary of in situ permeability measurements both within and outside the deformation zone.

Table S2. K-Ar data for the gouge samples of the Sibillini Mts. Thrust.

METHODS

- (1) We performed a detailed geological-structural mapping at the 1:5.000 scale of an area of about 2 km² as part of a broader geological mapping project covering the whole Mt. Sibilla-Mt. Priora area (about 15 km²) to reconstruct surface and subsurface geometries. The rocks are described and mapped based essentially on their lithological and micropalaeontological characteristics. Mapped structural elements consist of folds, faults, shear (C and C') and solution (S) planes of S-C/C' fabric, slickenlines and slickenfibers ([Ramsay & Graham, 1970](#); [Angelier, 1984](#)). The orientation of the faults and foliations of S-C/C' fabrics is plotted in equal-area Schmidt diagrams. Most of the key outcrops analysed in this works are located within a ca. 300 m long tunnel (Fig. 2). Geological mapping forms the basis for the meso-structural analysis of key exposures to reconstruct the architecture of the deformation zone and for the well-informed sampling strategy followed to select the most representative samples;
- (2) Detailed meso-structural analysis in the studied area and collection of representative samples. The meso-structural analysis was performed in order to reconstruct the geometry and kinematics of the whole study area;
- (3) Microstructural analysis of fault rocks by means of a high-resolution scanner and optical microscopy to infer the deformation mechanisms. We prepared 15 polished thin sections of the fault rocks and principal slip surfaces. We conducted observations under optical microscope (ZEISS AXIOSKOP-40) at Sapienza University of Rome to investigate the deformation mechanisms;
- (4) In situ air permeability measurements have been performed within the deformation zone (parallel and perpendicular to S-C tectonite, PSS, and footwall lenses) and out of the deformation zone (both parallel and perpendicular to S₀). Superficial alterations, when

present, have been carefully removed or avoided. In-situ permeability measurements have been carried out with a New England Research TinyPerm-3 air-minipermeameter calibrated by the manufacturer with known standards. The instrument allows a reliable field investigation of rock permeability within small volumes ($1\text{--}1.5\text{ cm}^3$) in the $10^{-3}\text{--}10^1$ Darcy (D) range, even though controlled laboratory tests have demonstrated its capability to measure permeability values as low as 10^{-5} D ([Filomena et al., 2014](#)). In the bulk-rock permeability mode, the air-minipermeameter directly yields an estimate of the permeability based on the outgoing air flow rate from the built-in compression vessel. Permeability values obtained from air-minipermeametry need to be corrected and standardized to be comparable with permeability values obtained from laboratory tests on rock plugs or image analysis ([Fossen et al., 2011](#); [Filomena et al., 2014](#); [Torabi et al., 2018](#)). In detail, air-minipermeameters yield either larger permeability values (by a factor of ca. 1.7) when compared with results derived from image analysis quantifications ([Fossen et al., 2011](#)), or lower permeabilities (-37%) than those obtained from small (<10 cm) rock plugs used in laboratory tests ([Filomena et al., 2014](#)). Hence, we use our data to understand the magnitude order of permeability differences between different tectonic structures within the deformation zones. Permeability results are listed in Table S1.

- (5) X-ray diffraction (XRD) analysis of two fault gouge samples were performed to define their mineralogical assemblage. XRD analyses were carried out by a Scintag X1 X-ray system (CuK α radiation) at 40 kV and 30 mA. Randomly oriented whole-rock powders were run in the $2\text{--}70^\circ$ 2θ interval with a step size of 0.05° 2θ and a counting time of 3 s per step. Standard patterns for illite 1M, and 2M₁ polytypes were represented by the pure illites RM30 and SG4 ([Eberl et al., 1987](#)), respectively. The occurrence of illite 1M polytype was confirmed by the

reflection peaks at 4.12, 3.68, and 3.07 Å (Fig. S2). Standard patterns for illite polytypes are stored into the Rockjock software ([Środoń et al. 2001](#); [Eberl 2003](#)) that fits the sum of XRD patterns of standards (calculated pattern) to the measured pattern by varying the fraction of each standard pattern. Integrated peak areas of clay minerals and illite polytype reflections were transformed into mineral concentration by using mineral intensity factors from Rockjock as a calibration constant (for a review, see [Moore and Reynolds, 1997](#)). The estimated quantification error is $\pm 5\%$. The peaks of non-clay minerals such as calcite, partially interfere with illite polytype peaks (e.g., 3.88 Å), modifying their heights and shapes. Such interference was taken into account when calculating integrated peak areas of clay minerals.

- (6) K-Ar geochronology of authigenic and syn-kinematic clay minerals from two fault gouge samples to constrain the timing of thrusting. Clay sample preparation and K-Ar dating was performed at the Geological Survey of Norway (NGU), Trondheim, following the standard analytical procedure for separating, characterizing, and dating fault gouges at the NGU Lab. Untreated fault sample material was weighed and loaded into HD-PE plastic bottle and Type II pure water (15 MΩ resistivity) was added to fully submerge the samples. The bottles were submerged in a Julabo F38-ME cryostatic bath filled with ethylene glycol, and subjected to at least 1 month of cyclic temperature oscillation between -12 °C and +25 °C with a 2 hour hold time at each temperature (>100 cycles). This allowed water to infiltrate between the particles and disaggregate them gently by gelification, without resulting in artificial grain size reduction. Subsequently, the finer than sand fractions of the samples were transferred to graduated cylinders using Type II pure water, and the <2 µm, 2–6 µm, and 6–10 µm fractions were successively extracted using Stokes' law. Two or more successive separations were performed to increase the yield of the <2 µm fraction.

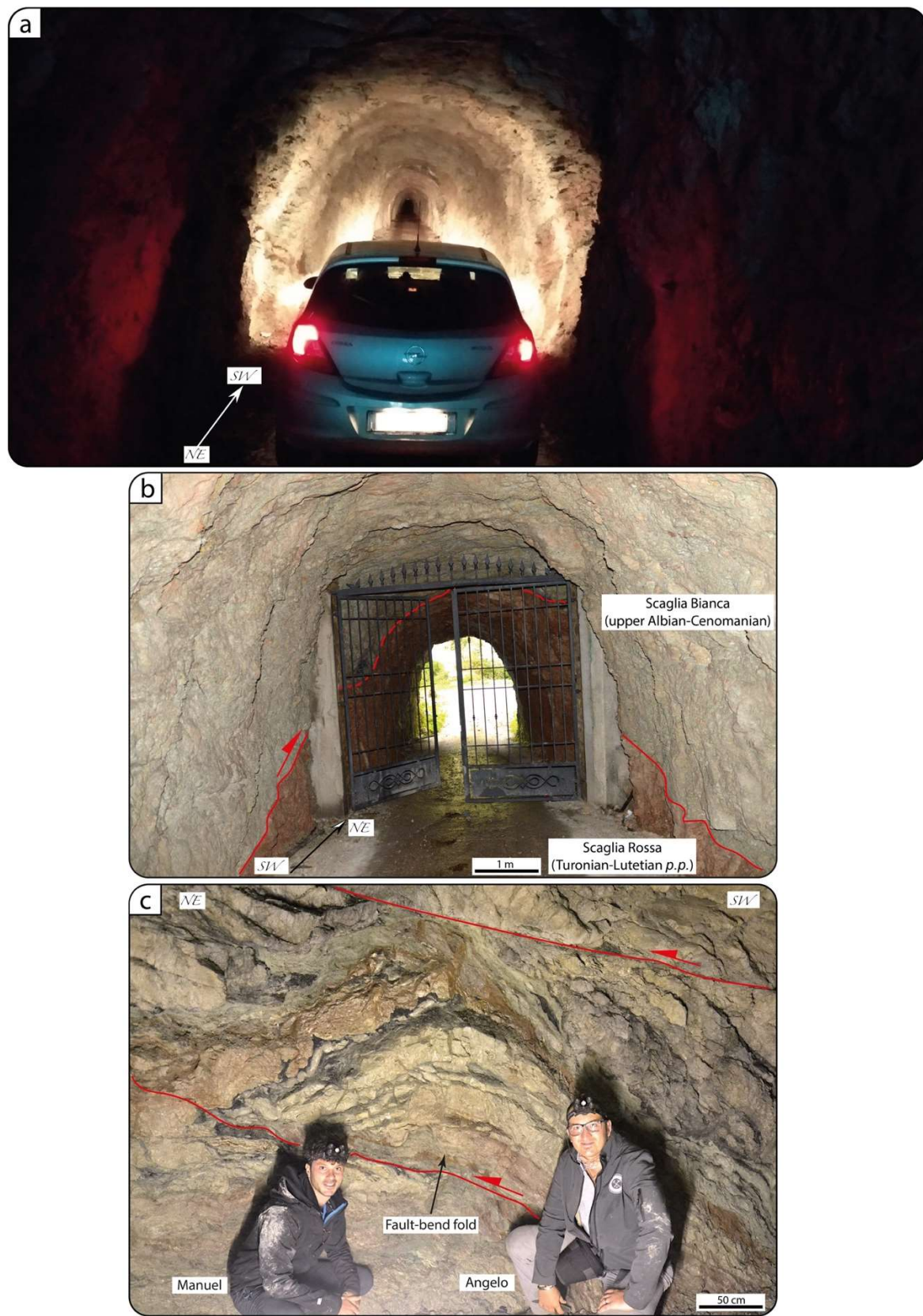
The <2 µm suspensions were centrifuged with a Beckman-Coulter Avanti J-26S XP centrifuge fitted with a JCF-Z continuous flow rotor and a calibrated Cole Parmer peristaltic pump, to separate 0.1–0.4 µm and <0.1 µm fractions. To generate <0.4 µm solutions, the centrifuge was run at 3700 RPM with a suspension flow-through rate of 400 ml/min, resulting in <0.4 µm supernatant suspensions and 0.4–2 µm solid pellets. The <0.4-µm suspensions were then centrifuged at 10.000 RPM with a solution flow-through rate of 180 ml/min to generate <0.1 µm supernatant suspensions and 0.1–0.4 µm solid pellets. The <0.1 µm supernatants were subsequently collected by centrifugation in a Beckman-Coulter Avanti J-26S XP centrifuge equipped with a JA-10 rotor, at 9500 RPM for 65 min, to collect the remaining <0.1 µm fractions as solid pellets. The <0.1 µm, 0.1–0.4 µm, 0.4–2 µm, 2–6 µm, and 6–10 µm grain size fractions were dried in an oven at 45 ± 10 °C. The centrifugation routine was calibrated and checked using LPS-PIDS with a Beckman Coulter LS13-320 particle size analyzer fitted with an aqueous liquid module. Air-dried, homogenized clay materials and standards were wrapped in folded molybdenum microcapsules, and the net mass of the aliquots was determined using a Mettler Toledo XPE26DR microbalance equipped with an antistatic ionizer. The microbalance has resolution of 2 µg and a measured uncertainty of 4 µg (1σ) for the total weighing procedure. The clays and standards were left overnight in a drying oven at 85 ± 3 °C and weighed again to determine the dry weight and relative humidity loss. The molybdenum envelopes were subsequently loaded into an ultrahigh vacuum extraction line and baked at a maximum temperature of 120 °C to eliminate excess water following the recommendations of [Clauer & Chaudhuri \(1995\)](#).

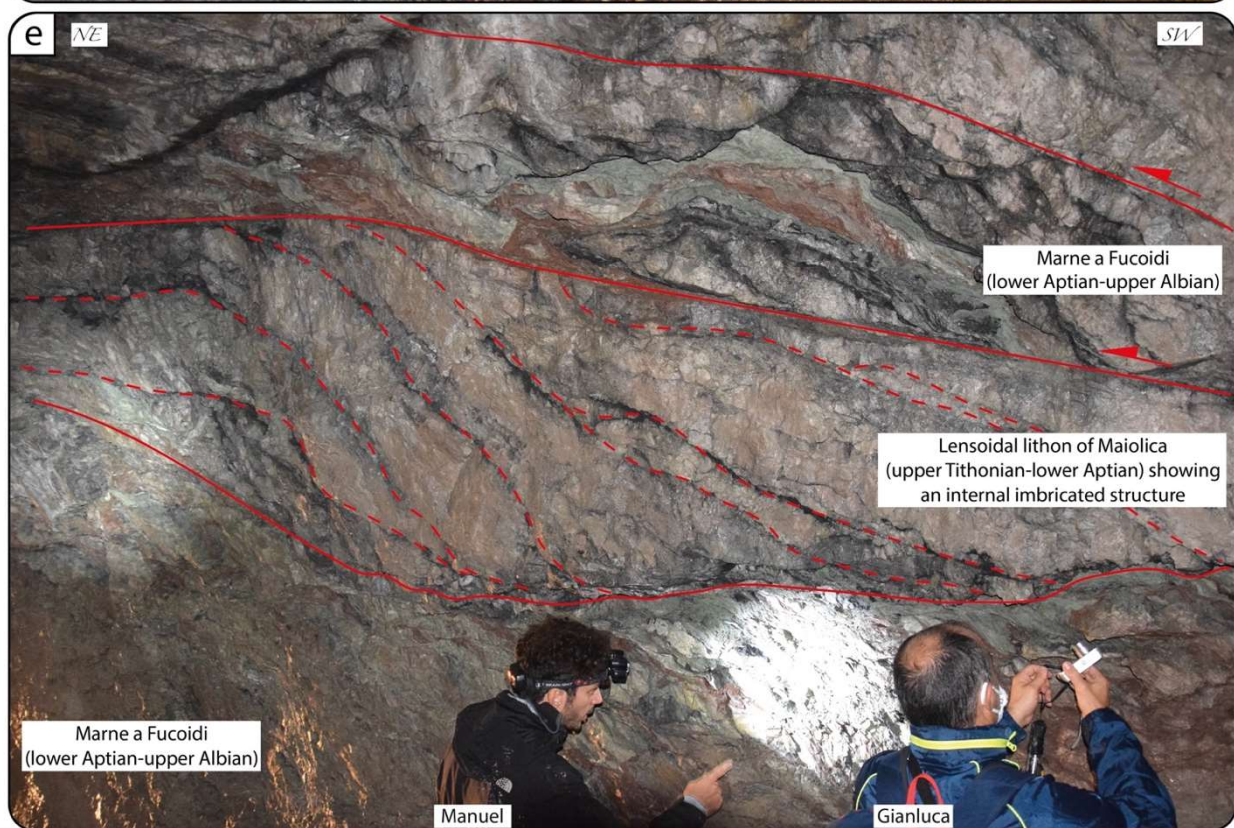
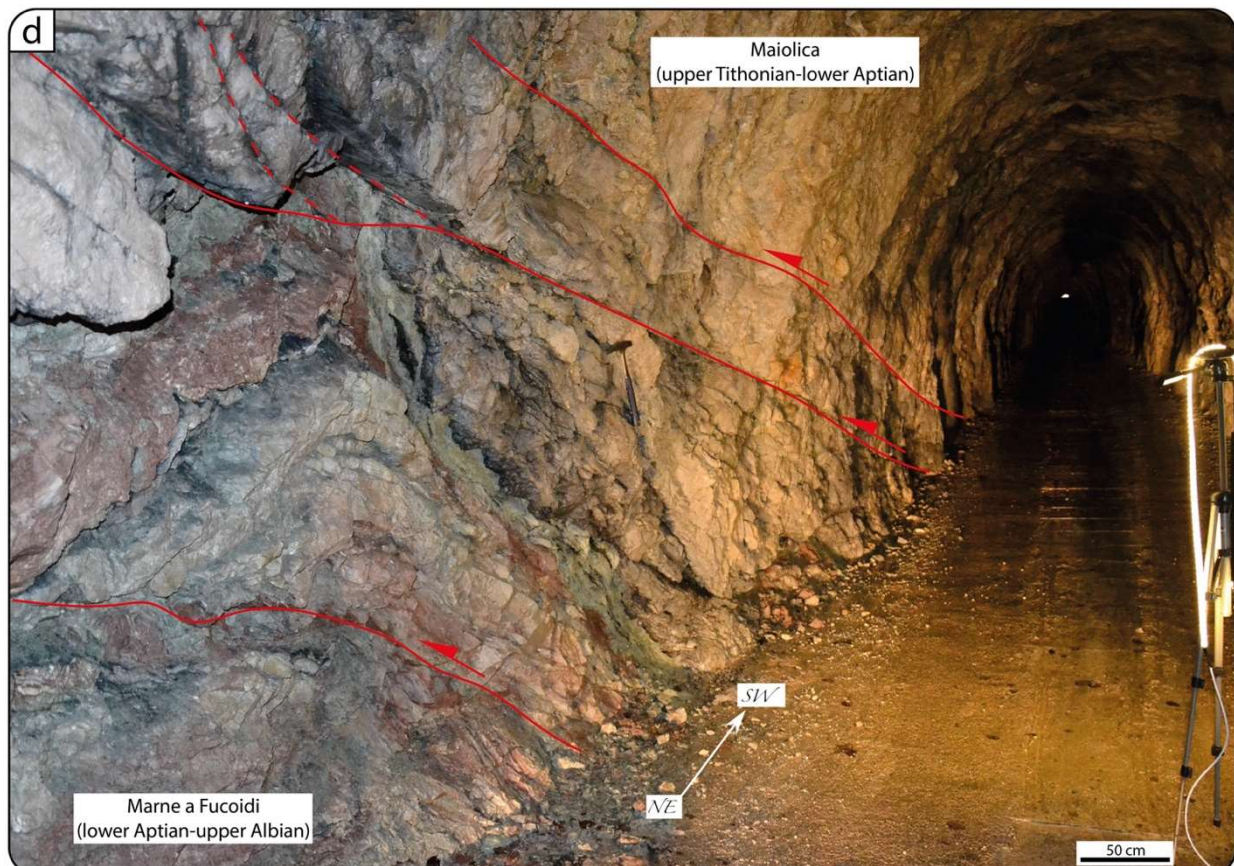
Argon was extracted from the samples in a Pond Engineering double vacuum resistance furnace at 1400 °C for 20 min. During heating, bulk sample gas was expanded directly into a

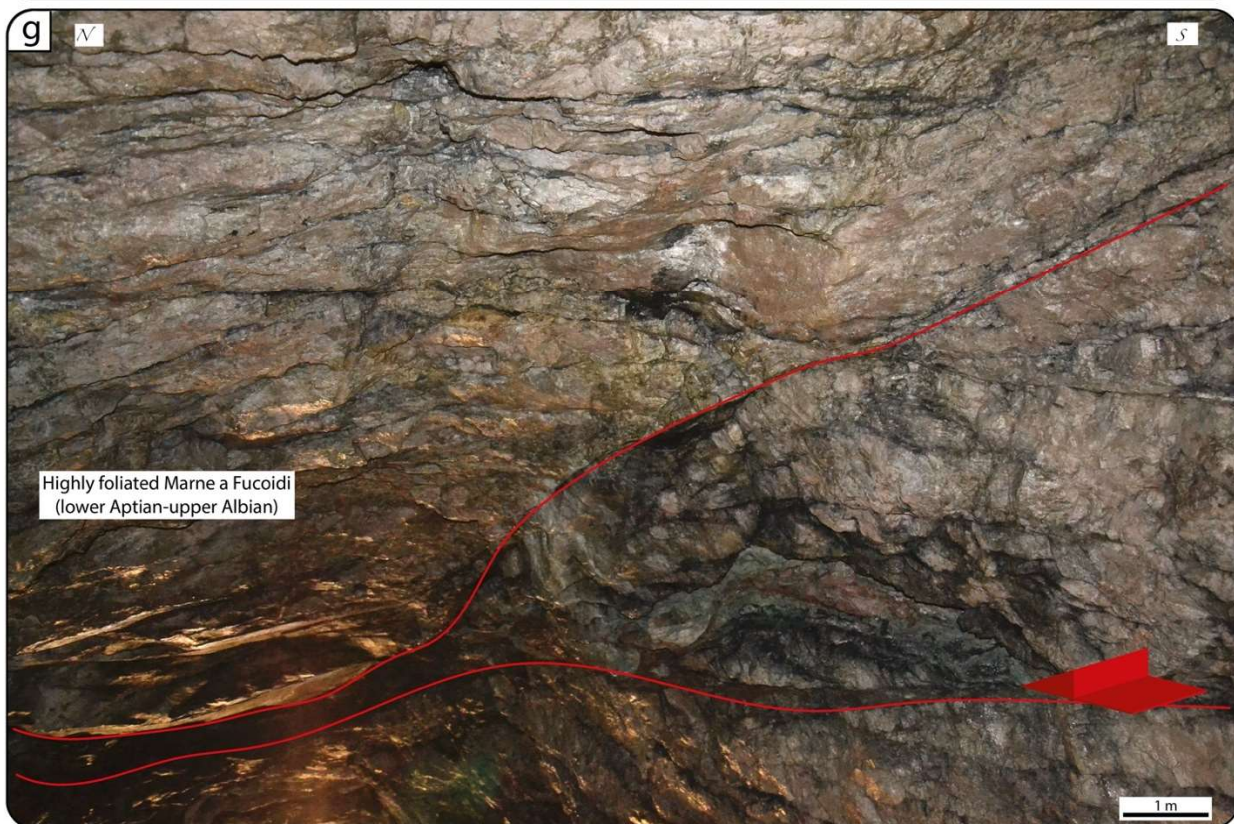
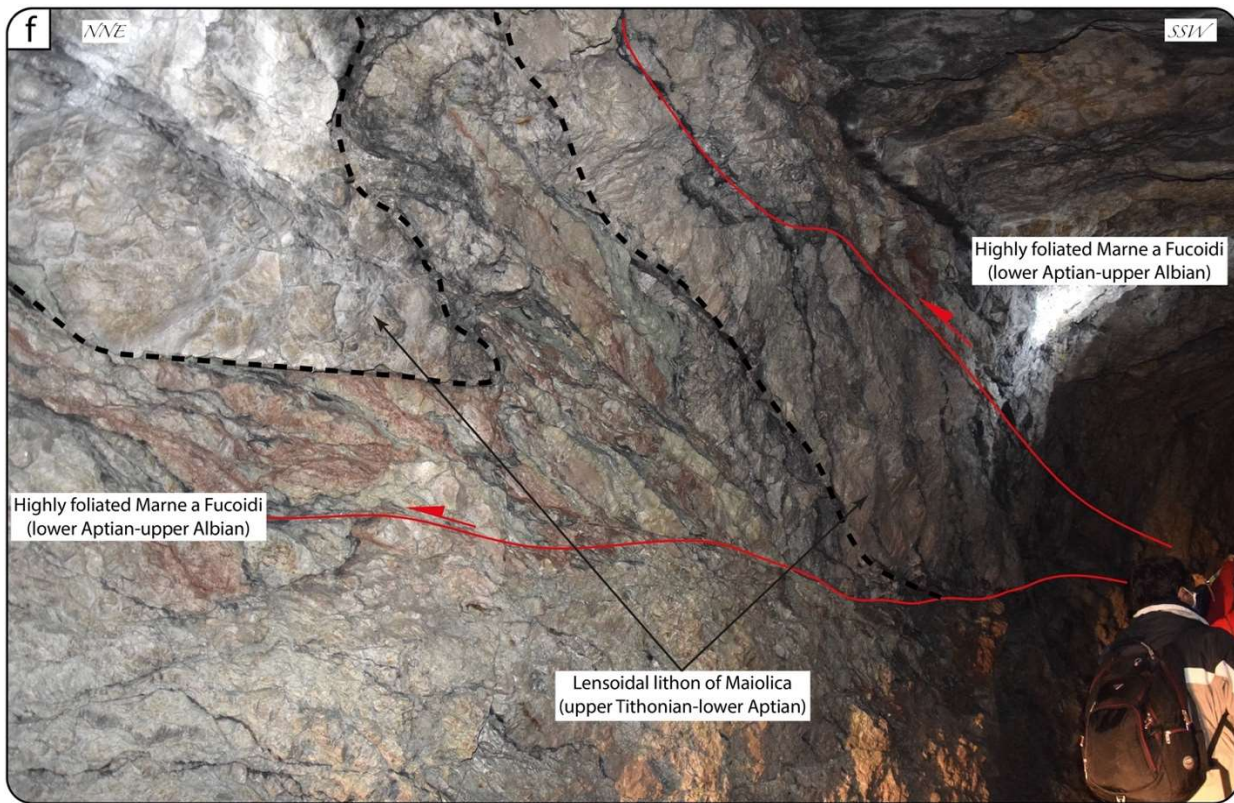
stainless steel vessel housing a freshly activated Titanium Sublimation Pump, to strip the sample gas from a majority of reactive gases including H₂O, N, O₂, CO, and CO₂. A known molar amount of approximately 2×10^{13} moles of pure ³⁸Ar spike ([Schumacher, 1975](#)) was prepared using a 0.2 cc gas pipette attached to a 4000 cc reservoir and was equilibrated with the purified sample gas. The gas mixture was subsequently isolated in a second clean-up stage and exposed for 10 min to two SAES GP50 getter cartridges with ST101 Zr-Al alloy, one of which was kept at 350 °C and one at room temperature, to remove residual reactive gases including H₂ and CH₄. Argon isotopes ratios were determined on an IsotopX NGX multicollector noble gas mass spectrometer in multicollector mode. Faraday cups with $10^{12} \Omega$ amplifiers were used to measure ³⁶Ar and ³⁸Ar, and a faraday cup with a $10^{11} \Omega$ amplifier was used to measure ⁴⁰Ar. Time-zero beam intensities were measured for 30 cycles of twenty 1-s integrations, and time-zero intensities were calculated using exponential regressions back to gas inlet time. Furnace blanks were run regularly between samples and had ⁴⁰Ar/³⁶Ar compositions close to atmospheric argon ([Lee et al., 2006](#)). Instrument mass discrimination was determined using aliquots of argon purified from air and compared with the reference value of 298.56 ± 0.31 ([Lee et al., 2006](#)). The ³⁸Ar spike pipette was calibrated using GA-1550 biotite with ⁴⁰Ar* = $1.342 \pm 0.007 \times 10^9$ mol/g (McDougall and Wellman, 2011) and HD-B1 biotite ([Fuhrmann et al., 1987, 1987](#)) with a ⁴⁰Ar* = $3.351 \pm 0.01 \times 10^{-10}$ mol/g. The overall standard deviation of the pooled spike calibrations by combined GA1550 and HD-B1 is <0.3%. The accuracy of the ⁴⁰Ar* determinations was monitored within run by GA-1550 and HD-B1 biotite. K concentration was determined by digesting a sample aliquot of ~5.5–50 mg in Li₂B₄O₇ flux at a temperature of 1000 ± 50 °C in Pd crucibles. The resulting glass was subsequently dissolved in HNO₃ and analyzed on a Perkin Elmer Optima 4300 DV ICP-

OES. 1σ uncertainties are estimated from the reproducibility of a range of standards with K concentrations between 0.19% K and 8.3% K and take into account the signal strength of K during analysis. Mean standard deviations of all measured standards overlap with published reference values within their published uncertainties. K-Ar ages were calculated using the 40K decay constants, abundance, and branching ratio of [Steiger & Jäger \(1977\)](#). Atmospheric Ar corrections were performed using the relative abundances of ^{40}Ar , ^{38}Ar and ^{36}Ar of [Lee et al. \(2006\)](#).

Figure S1.







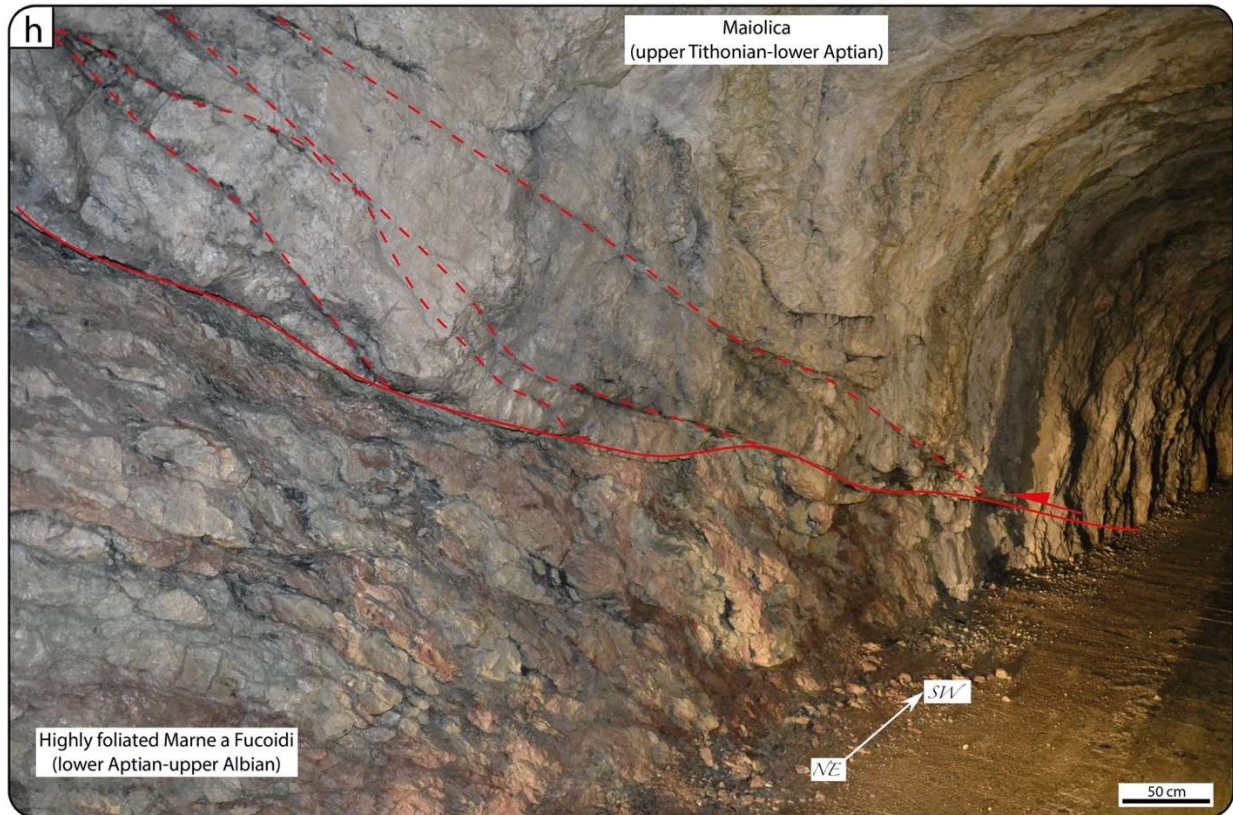


Figure S2.

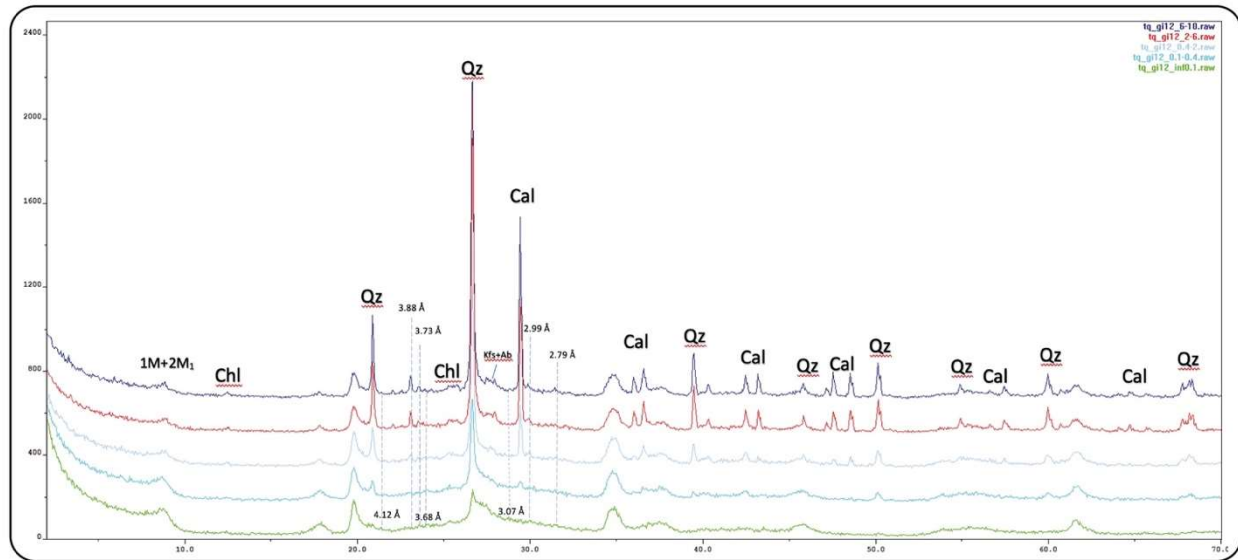


Table S1. Summary of in situ permeability measurements both within and outside the deformation zone

Structural station n° 1. Measurements orthogonal to S-C tectonite		
Number	Permeability (D)	Coordinates (UTM WGS84)
1	2,6E-02	42°55'29.07"N, 13°16'52.19"E
2	2,2E-03	42°55'29.07"N, 13°16'52.19"E
3	8,2E-02	42°55'29.07"N, 13°16'52.19"E
4	2,5E-04	42°55'29.07"N, 13°16'52.19"E
5	5,1E-04	42°55'29.07"N, 13°16'52.19"E
6	1,2E-02	42°55'29.07"N, 13°16'52.19"E
7	8,3E-02	42°55'29.07"N, 13°16'52.19"E
8	9,4E-04	42°55'29.07"N, 13°16'52.19"E
9	9,4E-05	42°55'29.07"N, 13°16'52.19"E
10	5,0E-03	42°55'29.07"N, 13°16'52.19"E
11	7,7E-02	42°55'29.07"N, 13°16'52.19"E
12	1,1E-03	42°55'29.07"N, 13°16'52.19"E
13	1,7E-02	42°55'29.07"N, 13°16'52.19"E
14	1,5E-03	42°55'29.07"N, 13°16'52.19"E
15	5,8E-03	42°55'29.07"N, 13°16'52.19"E
16	5,8E-03	42°55'29.07"N, 13°16'52.19"E
17	7,7E-04	42°55'29.07"N, 13°16'52.19"E
18	4,1E-04	42°55'29.07"N, 13°16'52.19"E
19	1,1E-03	42°55'29.07"N, 13°16'52.19"E
20	8,3E-02	42°55'29.07"N, 13°16'52.19"E
21	4,8E-03	42°55'29.07"N, 13°16'52.19"E
22	5,0E-03	42°55'29.07"N, 13°16'52.19"E
23	6,8E-04	42°55'29.07"N, 13°16'52.19"E
24	1,6E-01	42°55'29.07"N, 13°16'52.19"E
25	5,5E-04	42°55'29.07"N, 13°16'52.19"E
26	4,7E-05	42°55'29.07"N, 13°16'52.19"E
27	1,8E-03	42°55'29.07"N, 13°16'52.19"E
28	1,3E-02	42°55'29.07"N, 13°16'52.19"E
29	4,4E-03	42°55'29.07"N, 13°16'52.19"E
Structural station n° 1. Measurements parallel to S-C tectonite		
Number	Permeability (D)	Coordinates (UTM WGS84)
1	2,2E+00	42°55'29.07"N, 13°16'52.19"E
2	1,7E+00	42°55'29.07"N, 13°16'52.19"E
3	1,9E-01	42°55'29.07"N, 13°16'52.19"E
4	2,6E+00	42°55'29.07"N, 13°16'52.19"E
5	9,8E-01	42°55'29.07"N, 13°16'52.19"E
6	5,6E-01	42°55'29.07"N, 13°16'52.19"E
7	1,2E+00	42°55'29.07"N, 13°16'52.19"E
8	4,3E-01	42°55'29.07"N, 13°16'52.19"E
9	8,3E-01	42°55'29.07"N, 13°16'52.19"E
10	1,7E-01	42°55'29.07"N, 13°16'52.19"E
11	5,7E-01	42°55'29.07"N, 13°16'52.19"E
12	4,1E-01	42°55'29.07"N, 13°16'52.19"E
13	1,0E+00	42°55'29.07"N, 13°16'52.19"E
14	1,7E-01	42°55'29.07"N, 13°16'52.19"E
15	9,9E-03	42°55'29.07"N, 13°16'52.19"E
16	1,5E-01	42°55'29.07"N, 13°16'52.19"E
17	1,9E-01	42°55'29.07"N, 13°16'52.19"E
18	9,1E-02	42°55'29.07"N, 13°16'52.19"E
19	2,8E+00	42°55'29.07"N, 13°16'52.19"E
20	1,8E-01	42°55'29.07"N, 13°16'52.19"E
21	8,4E-02	42°55'29.07"N, 13°16'52.19"E
22	3,2E-01	42°55'29.07"N, 13°16'52.19"E
23	1,5E+00	42°55'29.07"N, 13°16'52.19"E
24	5,6E-01	42°55'29.07"N, 13°16'52.19"E

25	8,6E-02	42°55'29.07''N, 13°16'52.19''E
Structural station n° 2. Measurements orthogonal to S-C tectonite		
Number	Permeability (D)	Coordinates (UTM WGS84)
1	1,8E-02	42°55'25.15''N, 13°16'49.76''E
2	4,9E-02	42°55'25.15''N, 13°16'49.76''E
3	3,3E-01	42°55'25.15''N, 13°16'49.76''E
4	4,7E-02	42°55'25.15''N, 13°16'49.76''E
5	5,3E-03	42°55'25.15''N, 13°16'49.76''E
6	8,0E-03	42°55'25.15''N, 13°16'49.76''E
7	9,3E-03	42°55'25.15''N, 13°16'49.76''E
8	8,0E-03	42°55'25.15''N, 13°16'49.76''E
9	8,6E-03	42°55'25.15''N, 13°16'49.76''E
10	3,7E-03	42°55'25.15''N, 13°16'49.76''E
11	4,3E-03	42°55'25.15''N, 13°16'49.76''E
12	2,1E-03	42°55'25.15''N, 13°16'49.76''E
13	4,4E-04	42°55'25.15''N, 13°16'49.76''E
14	6,9E-03	42°55'25.15''N, 13°16'49.76''E
15	3,5E-02	42°55'25.15''N, 13°16'49.76''E
16	5,7E-03	42°55'25.15''N, 13°16'49.76''E
17	5,5E-03	42°55'25.15''N, 13°16'49.76''E
18	3,4E-02	42°55'25.15''N, 13°16'49.76''E
19	8,4E-03	42°55'25.15''N, 13°16'49.76''E
20	1,2E-01	42°55'25.15''N, 13°16'49.76''E
21	2,4E-02	42°55'25.15''N, 13°16'49.76''E
22	5,4E-03	42°55'25.15''N, 13°16'49.76''E
23	8,0E-03	42°55'25.15''N, 13°16'49.76''E
24	1,3E-04	42°55'25.15''N, 13°16'49.76''E
25	4,2E-02	42°55'25.15''N, 13°16'49.76''E
26	1,8E-02	42°55'25.15''N, 13°16'49.76''E
27	5,1E-03	42°55'25.15''N, 13°16'49.76''E
28	5,8E-03	42°55'25.15''N, 13°16'49.76''E
Structural station n° 2. Measurements parallel to S-C tectonite		
Number	Permeability (D)	Coordinates (UTM WGS84)
1	3,0E-01	42°55'25.15''N, 13°16'49.76''E
2	4,0E-01	42°55'25.15''N, 13°16'49.76''E
3	3,2E+00	42°55'25.15''N, 13°16'49.76''E
4	1,5E+00	42°55'25.15''N, 13°16'49.76''E
5	1,5E+00	42°55'25.15''N, 13°16'49.76''E
6	4,6E-01	42°55'25.15''N, 13°16'49.76''E
7	2,7E-01	42°55'25.15''N, 13°16'49.76''E
8	1,7E+00	42°55'25.15''N, 13°16'49.76''E
9	3,4E-01	42°55'25.15''N, 13°16'49.76''E
10	2,8E-01	42°55'25.15''N, 13°16'49.76''E
11	7,2E-02	42°55'25.15''N, 13°16'49.76''E
12	1,7E+00	42°55'25.15''N, 13°16'49.76''E
13	1,6E+00	42°55'25.15''N, 13°16'49.76''E
14	5,3E-03	42°55'25.15''N, 13°16'49.76''E
15	4,3E-01	42°55'25.15''N, 13°16'49.76''E
16	9,6E-01	42°55'25.15''N, 13°16'49.76''E
17	3,6E+00	42°55'25.15''N, 13°16'49.76''E
18	4,6E+00	42°55'25.15''N, 13°16'49.76''E
19	9,8E-01	42°55'25.15''N, 13°16'49.76''E
20	2,3E+00	42°55'25.15''N, 13°16'49.76''E
21	1,9E+00	42°55'25.15''N, 13°16'49.76''E
22	2,5E+00	42°55'25.15''N, 13°16'49.76''E
23	3,2E+00	42°55'25.15''N, 13°16'49.76''E
24	3,9E+00	42°55'25.15''N, 13°16'49.76''E
25	1,6E+00	42°55'25.15''N, 13°16'49.76''E

26	5,9E-02	42°55'25.15''N, 13°16'49.76''E
27	7,8E-01	42°55'25.15''N, 13°16'49.76''E
Structural station n° 3. Measurements orthogonal to S-C tectonite		
Number	Permeability (D)	Coordinates (UTM WGS84)
1	1,2E-04	42°55'15.25''N, 13°16'44.36''E
2	5,1E-02	42°55'15.25''N, 13°16'44.36''E
3	3,2E-03	42°55'15.25''N, 13°16'44.36''E
4	5,0E-04	42°55'15.25''N, 13°16'44.36''E
5	4,2E-04	42°55'15.25''N, 13°16'44.36''E
6	2,9E-01	42°55'15.25''N, 13°16'44.36''E
7	1,3E-03	42°55'15.25''N, 13°16'44.36''E
8	1,5E-03	42°55'15.25''N, 13°16'44.36''E
9	1,6E-03	42°55'15.25''N, 13°16'44.36''E
10	1,0E-03	42°55'15.25''N, 13°16'44.36''E
11	5,4E-02	42°55'15.25''N, 13°16'44.36''E
12	1,7E-04	42°55'15.25''N, 13°16'44.36''E
13	1,3E-03	42°55'15.25''N, 13°16'44.36''E
14	5,5E-02	42°55'15.25''N, 13°16'44.36''E
15	2,6E-04	42°55'15.25''N, 13°16'44.36''E
16	5,1E-02	42°55'15.25''N, 13°16'44.36''E
17	4,5E-05	42°55'15.25''N, 13°16'44.36''E
18	2,4E-03	42°55'15.25''N, 13°16'44.36''E
19	5,5E-02	42°55'15.25''N, 13°16'44.36''E
20	3,3E-05	42°55'15.25''N, 13°16'44.36''E
21	4,5E-02	42°55'15.25''N, 13°16'44.36''E
22	9,6E-03	42°55'15.25''N, 13°16'44.36''E
23	6,1E-05	42°55'15.25''N, 13°16'44.36''E
24	5,3E-02	42°55'15.25''N, 13°16'44.36''E
25	6,8E-02	42°55'15.25''N, 13°16'44.36''E
26	1,1E-03	42°55'15.25''N, 13°16'44.36''E
27	3,7E-04	42°55'15.25''N, 13°16'44.36''E
28	1,6E-01	42°55'15.25''N, 13°16'44.36''E
29	5,7E-02	42°55'15.25''N, 13°16'44.36''E
Structural station n° 3. Measurements parallel to S-C tectonite		
Number	Permeability (D)	Coordinates (UTM WGS84)
1	1,5E+00	42°55'15.25''N, 13°16'44.36''E
2	4,1E-01	42°55'15.25''N, 13°16'44.36''E
3	1,0E-01	42°55'15.25''N, 13°16'44.36''E
4	3,0E-01	42°55'15.25''N, 13°16'44.36''E
5	8,6E-02	42°55'15.25''N, 13°16'44.36''E
6	1,4E-01	42°55'15.25''N, 13°16'44.36''E
7	1,3E+00	42°55'15.25''N, 13°16'44.36''E
8	4,1E-01	42°55'15.25''N, 13°16'44.36''E
9	1,5E-01	42°55'15.25''N, 13°16'44.36''E
10	9,4E-01	42°55'15.25''N, 13°16'44.36''E
11	1,3E-02	42°55'15.25''N, 13°16'44.36''E
12	4,0E-01	42°55'15.25''N, 13°16'44.36''E
13	9,6E-01	42°55'15.25''N, 13°16'44.36''E
14	1,4E+00	42°55'15.25''N, 13°16'44.36''E
15	6,1E-02	42°55'15.25''N, 13°16'44.36''E
16	8,9E-02	42°55'15.25''N, 13°16'44.36''E
17	7,1E-01	42°55'15.25''N, 13°16'44.36''E
18	4,3E-01	42°55'15.25''N, 13°16'44.36''E
19	1,8E-01	42°55'15.25''N, 13°16'44.36''E
20	4,5E-03	42°55'15.25''N, 13°16'44.36''E
21	1,8E-01	42°55'15.25''N, 13°16'44.36''E
22	1,0E-01	42°55'15.25''N, 13°16'44.36''E
23	1,1E-01	42°55'15.25''N, 13°16'44.36''E

24	1,4E+00	42°55'15.25"N, 13°16'44.36"E
25	1,4E-01	42°55'15.25"N, 13°16'44.36"E
26	5,1E-02	42°55'15.25"N, 13°16'44.36"E
27	3,4E-01	42°55'15.25"N, 13°16'44.36"E
28	2,7E-01	42°55'15.25"N, 13°16'44.36"E
29	1,4E-03	42°55'15.25"N, 13°16'44.36"E

Structural station n° 4. Measurements orthogonal to S-C tectonite

Number	Permeability (D)	Coordinates (UTM WGS84)
1	2,0E-03	42°55'16.84"N, 13°16'42.78"E
2	6,4E-02	42°55'16.84"N, 13°16'42.78"E
3	6,3E-04	42°55'16.84"N, 13°16'42.78"E
4	5,4E-04	42°55'16.84"N, 13°16'42.78"E
5	1,8E-03	42°55'16.84"N, 13°16'42.78"E
6	1,5E-02	42°55'16.84"N, 13°16'42.78"E
7	3,0E-03	42°55'16.84"N, 13°16'42.78"E
8	7,1E-02	42°55'16.84"N, 13°16'42.78"E
9	5,4E-03	42°55'16.84"N, 13°16'42.78"E
10	6,0E-02	42°55'16.84"N, 13°16'42.78"E
11	2,9E-03	42°55'16.84"N, 13°16'42.78"E
12	6,4E-02	42°55'16.84"N, 13°16'42.78"E
13	4,5E-04	42°55'16.84"N, 13°16'42.78"E
14	6,3E-02	42°55'16.84"N, 13°16'42.78"E
15	7,1E-02	42°55'16.84"N, 13°16'42.78"E
16	2,4E-02	42°55'16.84"N, 13°16'42.78"E
17	1,9E-01	42°55'16.84"N, 13°16'42.78"E
18	8,1E-02	42°55'16.84"N, 13°16'42.78"E
19	2,5E-01	42°55'16.84"N, 13°16'42.78"E
20	6,5E-02	42°55'16.84"N, 13°16'42.78"E
21	6,6E-02	42°55'16.84"N, 13°16'42.78"E
22	8,9E-03	42°55'16.84"N, 13°16'42.78"E
23	1,9E-01	42°55'16.84"N, 13°16'42.78"E

Structural station n° 4. Measurements parallel to S-C tectonite

Number	Permeability (D)	Coordinates (UTM WGS84)
1	3,1E-02	42°55'16.84"N, 13°16'42.78"E
2	7,9E-02	42°55'16.84"N, 13°16'42.78"E
3	6,2E-01	42°55'16.84"N, 13°16'42.78"E
4	2,1E+00	42°55'16.84"N, 13°16'42.78"E
5	1,4E-01	42°55'16.84"N, 13°16'42.78"E
6	7,4E-02	42°55'16.84"N, 13°16'42.78"E
7	7,4E-04	42°55'16.84"N, 13°16'42.78"E
8	9,5E-01	42°55'16.84"N, 13°16'42.78"E
9	1,3E-01	42°55'16.84"N, 13°16'42.78"E
10	1,1E-03	42°55'16.84"N, 13°16'42.78"E
11	1,6E-03	42°55'16.84"N, 13°16'42.78"E
12	4,2E-02	42°55'16.84"N, 13°16'42.78"E
13	7,5E-02	42°55'16.84"N, 13°16'42.78"E
14	2,4E-02	42°55'16.84"N, 13°16'42.78"E
15	2,1E-01	42°55'16.84"N, 13°16'42.78"E
16	3,4E-01	42°55'16.84"N, 13°16'42.78"E
17	3,2E-01	42°55'16.84"N, 13°16'42.78"E
18	4,0E-01	42°55'16.84"N, 13°16'42.78"E
19	1,2E-04	42°55'16.84"N, 13°16'42.78"E
20	1,7E+00	42°55'16.84"N, 13°16'42.78"E
21	9,6E-04	42°55'16.84"N, 13°16'42.78"E
22	2,2E-01	42°55'16.84"N, 13°16'42.78"E
23	6,5E-01	42°55'16.84"N, 13°16'42.78"E
24	9,2E-05	42°55'16.84"N, 13°16'42.78"E
25	1,0E+00	42°55'16.84"N, 13°16'42.78"E

26	7,9E-02	42°55'16.84"N, 13°16'42.78"E
27	2,9E-01	42°55'16.84"N, 13°16'42.78"E
28	2,0E-01	42°55'16.84"N, 13°16'42.78"E

Structural station n° 4. Measurements parallel to foliation within calcareous lenses

Number	Permeability (D)	Coordinates (UTM WGS84)
1	7,0E-02	42°55'16.84"N, 13°16'42.78"E
2	5,1E-02	42°55'16.84"N, 13°16'42.78"E
3	1,1E-03	42°55'16.84"N, 13°16'42.78"E
4	3,8E-04	42°55'16.84"N, 13°16'42.78"E
5	2,6E-04	42°55'16.84"N, 13°16'42.78"E
6	1,3E-04	42°55'16.84"N, 13°16'42.78"E
7	5,5E-03	42°55'16.84"N, 13°16'42.78"E
8	1,9E-04	42°55'16.84"N, 13°16'42.78"E
9	8,9E-03	42°55'16.84"N, 13°16'42.78"E
10	4,5E-04	42°55'16.84"N, 13°16'42.78"E
11	3,3E-01	42°55'16.84"N, 13°16'42.78"E
12	6,3E-02	42°55'16.84"N, 13°16'42.78"E
13	6,1E-02	42°55'16.84"N, 13°16'42.78"E
14	4,9E-02	42°55'16.84"N, 13°16'42.78"E
15	3,4E-04	42°55'16.84"N, 13°16'42.78"E
16	3,5E-04	42°55'16.84"N, 13°16'42.78"E
17	9,5E-03	42°55'16.84"N, 13°16'42.78"E
18	7,2E-02	42°55'16.84"N, 13°16'42.78"E
19	7,0E-03	42°55'16.84"N, 13°16'42.78"E
20	5,4E-05	42°55'16.84"N, 13°16'42.78"E
21	9,2E-01	42°55'16.84"N, 13°16'42.78"E
22	5,0E-03	42°55'16.84"N, 13°16'42.78"E
23	8,9E-02	42°55'16.84"N, 13°16'42.78"E
24	6,9E-02	42°55'16.84"N, 13°16'42.78"E
25	1,8E-02	42°55'16.84"N, 13°16'42.78"E
26	4,1E-04	42°55'16.84"N, 13°16'42.78"E
27	6,9E-02	42°55'16.84"N, 13°16'42.78"E
28	7,2E-01	42°55'16.84"N, 13°16'42.78"E
29	6,8E-02	42°55'16.84"N, 13°16'42.78"E
30	1,4E-03	42°55'16.84"N, 13°16'42.78"E

Structural station n° 4. Measurements orthogonal to PSS

Number	Permeability (D)	Coordinates (UTM WGS84)
1	7,6E-02	42°55'16.84"N, 13°16'42.78"E
2	7,0E-02	42°55'16.84"N, 13°16'42.78"E
3	2,4E-02	42°55'16.84"N, 13°16'42.78"E
4	6,1E-02	42°55'16.84"N, 13°16'42.78"E
5	6,7E-02	42°55'16.84"N, 13°16'42.78"E
6	6,2E-02	42°55'16.84"N, 13°16'42.78"E
7	6,1E-02	42°55'16.84"N, 13°16'42.78"E
8	1,2E-01	42°55'16.84"N, 13°16'42.78"E
9	1,9E-04	42°55'16.84"N, 13°16'42.78"E
10	6,2E-02	42°55'16.84"N, 13°16'42.78"E
11	3,8E-04	42°55'16.84"N, 13°16'42.78"E
12	5,5E-05	42°55'16.84"N, 13°16'42.78"E
13	6,2E-02	42°55'16.84"N, 13°16'42.78"E
14	6,7E-02	42°55'16.84"N, 13°16'42.78"E
15	7,0E-01	42°55'16.84"N, 13°16'42.78"E
16	6,0E-02	42°55'16.84"N, 13°16'42.78"E
17	1,9E-03	42°55'16.84"N, 13°16'42.78"E
18	5,8E-02	42°55'16.84"N, 13°16'42.78"E
19	2,0E-02	42°55'16.84"N, 13°16'42.78"E
20	3,1E-05	42°55'16.84"N, 13°16'42.78"E
21	7,0E-02	42°55'16.84"N, 13°16'42.78"E

22	2,2E-04	42°55'16.84"N, 13°16'42.78"E
23	4,6E-04	42°55'16.84"N, 13°16'42.78"E
24	2,8E-04	42°55'16.84"N, 13°16'42.78"E
25	2,2E-02	42°55'16.84"N, 13°16'42.78"E
26	4,0E-04	42°55'16.84"N, 13°16'42.78"E
27	2,8E-04	42°55'16.84"N, 13°16'42.78"E
28	6,4E-02	42°55'16.84"N, 13°16'42.78"E
Structural station n° 4. Measurements parallel to foowall lenses of Maiolica cherty limestones		
Number	Permeability (D)	Coordinates (UTM WGS84)
1	-3,4E+00	42°55'16.84"N, 13°16'42.78"E
2	-3,2E+00	42°55'16.84"N, 13°16'42.78"E
3	-1,2E+00	42°55'16.84"N, 13°16'42.78"E
4	-1,5E+00	42°55'16.84"N, 13°16'42.78"E
5	-1,3E+00	42°55'16.84"N, 13°16'42.78"E
6	-5,4E-01	42°55'16.84"N, 13°16'42.78"E
7	-1,3E+00	42°55'16.84"N, 13°16'42.78"E
8	-2,9E+00	42°55'16.84"N, 13°16'42.78"E
9	-1,6E+00	42°55'16.84"N, 13°16'42.78"E
10	-9,0E-01	42°55'16.84"N, 13°16'42.78"E
11	-7,6E-01	42°55'16.84"N, 13°16'42.78"E
12	-1,2E+00	42°55'16.84"N, 13°16'42.78"E
13	-1,2E+00	42°55'16.84"N, 13°16'42.78"E
14	-3,3E+00	42°55'16.84"N, 13°16'42.78"E
15	-1,2E+00	42°55'16.84"N, 13°16'42.78"E
16	-1,3E+00	42°55'16.84"N, 13°16'42.78"E
17	-1,3E+00	42°55'16.84"N, 13°16'42.78"E
18	-3,6E+00	42°55'16.84"N, 13°16'42.78"E
19	-4,1E+00	42°55'16.84"N, 13°16'42.78"E
20	-3,2E+00	42°55'16.84"N, 13°16'42.78"E
21	-1,3E+00	42°55'16.84"N, 13°16'42.78"E
22	-1,3E+00	42°55'16.84"N, 13°16'42.78"E
23	-1,3E+00	42°55'16.84"N, 13°16'42.78"E
24	-1,3E+00	42°55'16.84"N, 13°16'42.78"E
25	-1,1E+00	42°55'16.84"N, 13°16'42.78"E
26	-5,0E-01	42°55'16.84"N, 13°16'42.78"E
27	-1,3E+00	42°55'16.84"N, 13°16'42.78"E
28	-1,3E+00	42°55'16.84"N, 13°16'42.78"E
29	-3,9E-01	42°55'16.84"N, 13°16'42.78"E
30	-1,3E+00	42°55'16.84"N, 13°16'42.78"E
31	-2,9E+00	42°55'16.84"N, 13°16'42.78"E
32	-1,3E+00	42°55'16.84"N, 13°16'42.78"E
33	-1,3E+00	42°55'16.84"N, 13°16'42.78"E
34	-1,3E+00	42°55'16.84"N, 13°16'42.78"E
35	-1,3E+00	42°55'16.84"N, 13°16'42.78"E
36	-1,2E+00	42°55'16.84"N, 13°16'42.78"E
37	-3,5E+00	42°55'16.84"N, 13°16'42.78"E
38	-3,1E+00	42°55'16.84"N, 13°16'42.78"E
39	-1,3E+00	42°55'16.84"N, 13°16'42.78"E
40	-1,3E+00	42°55'16.84"N, 13°16'42.78"E
41	-1,3E+00	42°55'16.84"N, 13°16'42.78"E
42	-3,9E+00	42°55'16.84"N, 13°16'42.78"E
43	-2,5E+00	42°55'16.84"N, 13°16'42.78"E
44	-1,2E+00	42°55'16.84"N, 13°16'42.78"E
45	-4,6E-01	42°55'16.84"N, 13°16'42.78"E
46	-2,5E+00	42°55'16.84"N, 13°16'42.78"E
47	-6,5E-01	42°55'16.84"N, 13°16'42.78"E
48	-3,1E+00	42°55'16.84"N, 13°16'42.78"E
49	-3,2E+00	42°55'16.84"N, 13°16'42.78"E

50	-1,1E+00	42°55'16.84"N, 13°16'42.78"E
51	-3,3E+00	42°55'16.84"N, 13°16'42.78"E
Measurement out of deformation zone – Parallel to S ₀ of Maiolica cherty limestones		
Number	Permeability (D)	Coordinates (UTM WGS84)
1	4,4E-04	42°54'20.49"N, 13°17'19.92"E
2	8,3E-02	42°54'20.49"N, 13°17'19.92"E
3	2,7E-04	42°54'20.49"N, 13°17'19.92"E
4	8,9E-02	42°54'20.49"N, 13°17'19.92"E
5	2,7E-04	42°54'20.49"N, 13°17'19.92"E
6	2,2E-03	42°54'20.49"N, 13°17'19.92"E
7	8,6E-02	42°54'20.49"N, 13°17'19.92"E
8	8,7E-02	42°54'20.49"N, 13°17'19.92"E
9	6,6E-02	42°54'20.49"N, 13°17'19.92"E
10	1,8E-04	42°54'20.49"N, 13°17'19.92"E
11	1,8E-03	42°54'20.49"N, 13°17'19.92"E
12	6,7E-02	42°54'20.49"N, 13°17'19.92"E
13	7,8E-02	42°54'20.49"N, 13°17'19.92"E
14	8,1E-04	42°54'20.49"N, 13°17'19.92"E
15	7,8E-02	42°54'20.49"N, 13°17'19.92"E
16	7,9E-02	42°54'20.49"N, 13°17'19.92"E
17	5,8E-02	42°54'20.49"N, 13°17'19.92"E
18	1,8E-02	42°54'20.49"N, 13°17'19.92"E
Measurement out of deformation zone – Orthogonal to S ₀ of Maiolica cherty limestones		
Number	Permeability (D)	Coordinates (UTM WGS84)
1	2,7E-03	42°54'20.49"N, 13°17'19.92"E
2	1,0E-01	42°54'20.49"N, 13°17'19.92"E
3	4,0E-02	42°54'20.49"N, 13°17'19.92"E
4	8,5E-05	42°54'20.49"N, 13°17'19.92"E
5	8,1E-02	42°54'20.49"N, 13°17'19.92"E
6	1,5E-02	42°54'20.49"N, 13°17'19.92"E
7	8,2E-02	42°54'20.49"N, 13°17'19.92"E
8	6,9E-02	42°54'20.49"N, 13°17'19.92"E
9	4,0E-04	42°54'20.49"N, 13°17'19.92"E
10	7,7E-02	42°54'20.49"N, 13°17'19.92"E
11	7,1E-02	42°54'20.49"N, 13°17'19.92"E
12	6,9E-04	42°54'20.49"N, 13°17'19.92"E
13	1,6E-04	42°54'20.49"N, 13°17'19.92"E
14	4,9E-02	42°54'20.49"N, 13°17'19.92"E
15	3,5E-03	42°54'20.49"N, 13°17'19.92"E
16	7,5E-02	42°54'20.49"N, 13°17'19.92"E
17	7,4E-02	42°54'20.49"N, 13°17'19.92"E
18	7,5E-02	42°54'20.49"N, 13°17'19.92"E
Measurement out of deformation zone – Parallel to S ₀ of Marne a Fucoidi marly limestones		
Number	Permeability (D)	Coordinates (UTM WGS84)
1	1,2E-01	42°53'49.86"N, 13°15'16.52"E
2	5,8E-01	42°53'49.86"N, 13°15'16.52"E
3	3,0E-03	42°53'49.86"N, 13°15'16.52"E
4	3,0E-04	42°53'49.86"N, 13°15'16.52"E
5	1,9E-03	42°53'49.86"N, 13°15'16.52"E
6	1,2E-03	42°53'49.86"N, 13°15'16.52"E
7	6,4E-04	42°53'49.86"N, 13°15'16.52"E
8	4,9E-01	42°53'49.86"N, 13°15'16.52"E
9	2,6E-03	42°53'49.86"N, 13°15'16.52"E
10	1,1E-03	42°53'49.86"N, 13°15'16.52"E
11	7,0E-02	42°53'49.86"N, 13°15'16.52"E
12	2,2E-01	42°53'49.86"N, 13°15'16.52"E
13	1,6E-01	42°53'49.86"N, 13°15'16.52"E
14	2,8E-02	42°53'49.86"N, 13°15'16.52"E

15	1,9E-02	42°53'49.86''N, 13°15'16.52''E
16	2,2E-02	42°53'49.86''N, 13°15'16.52''E
17	1,3E-02	42°53'49.86''N, 13°15'16.52''E
18	5,6E-03	42°53'49.86''N, 13°15'16.52''E
19	7,0E-03	42°53'49.86''N, 13°15'16.52''E
20	1,5E-01	42°53'49.86''N, 13°15'16.52''E

Measurement out of deformation zone – Orthogonal to S₀ of Marne a Fucoidi marly limestones

Number	Permeability (D)	Coordinates (UTM WGS84)
1	3,6E-04	42°53'49.86''N, 13°15'16.52''E
2	6,4E-04	42°53'49.86''N, 13°15'16.52''E
3	2,6E-03	42°53'49.86''N, 13°15'16.52''E
4	7,6E-02	42°53'49.86''N, 13°15'16.52''E
5	7,0E-02	42°53'49.86''N, 13°15'16.52''E
6	2,3E-03	42°53'49.86''N, 13°15'16.52''E
7	1,2E-02	42°53'49.86''N, 13°15'16.52''E
8	1,6E-03	42°53'49.86''N, 13°15'16.52''E
9	6,9E-02	42°53'49.86''N, 13°15'16.52''E
10	7,0E-02	42°53'49.86''N, 13°15'16.52''E
11	3,0E-01	42°53'49.86''N, 13°15'16.52''E
12	7,0E-01	42°53'49.86''N, 13°15'16.52''E
13	2,3E-01	42°53'49.86''N, 13°15'16.52''E
14	2,4E-04	42°53'49.86''N, 13°15'16.52''E
15	1,1E-03	42°53'49.86''N, 13°15'16.52''E
16	2,7E-03	42°53'49.86''N, 13°15'16.52''E
17	5,7E-04	42°53'49.86''N, 13°15'16.52''E
18	6,3E-04	42°53'49.86''N, 13°15'16.52''E
19	7,6E-02	42°53'49.86''N, 13°15'16.52''E
20	7,4E-02	42°53'49.86''N, 13°15'16.52''E

Measurement out of deformation zone – Parallel to S₀ of Scaglia Rossa limestones

Number	Permeability (D)	Coordinates (UTM WGS84)
1	2,9E-01	42°53'55.40''N, 13°15'31.30''E
2	1,2E-03	42°53'55.40''N, 13°15'31.30''E
3	5,6E-03	42°53'55.40''N, 13°15'31.30''E
4	7,0E-03	42°53'55.40''N, 13°15'31.30''E
5	6,8E-02	42°53'55.40''N, 13°15'31.30''E
6	1,4E-04	42°53'55.40''N, 13°15'31.30''E
7	5,8E-02	42°53'55.40''N, 13°15'31.30''E
8	7,1E-02	42°53'55.40''N, 13°15'31.30''E
9	1,1E-01	42°53'55.40''N, 13°15'31.30''E
10	4,1E-01	42°53'55.40''N, 13°15'31.30''E
11	4,1E-01	42°53'55.40''N, 13°15'31.30''E
12	1,2E-04	42°53'55.40''N, 13°15'31.30''E
13	7,0E-02	42°53'55.40''N, 13°15'31.30''E
14	1,6E-04	42°53'55.40''N, 13°15'31.30''E
15	6,8E-02	42°53'55.40''N, 13°15'31.30''E
16	7,3E-02	42°53'55.40''N, 13°15'31.30''E
17	5,1E-01	42°53'55.40''N, 13°15'31.30''E
18	7,0E-05	42°53'55.40''N, 13°15'31.30''E
19	3,8E-01	42°53'55.40''N, 13°15'31.30''E

Measurement out of deformation zone – Orthogonal to S₀ of Scaglia Rossa limestones

Number	Permeability (D)	Coordinates (UTM WGS84)
1	2,6E-02	42°53'55.40''N, 13°15'31.30''E
2	6,4E-02	42°53'55.40''N, 13°15'31.30''E
3	1,2E-04	42°53'55.40''N, 13°15'31.30''E
4	6,7E-02	42°53'55.40''N, 13°15'31.30''E
5	5,5E-05	42°53'55.40''N, 13°15'31.30''E
6	3,6E-03	42°53'55.40''N, 13°15'31.30''E
7	6,9E-02	42°53'55.40''N, 13°15'31.30''E

8	6,8E-02	42°53'55.40"N, 13°15'31.30"E
9	6,9E-02	42°53'55.40"N, 13°15'31.30"E
10	1,2E-01	42°53'55.40"N, 13°15'31.30"E
11	5,9E-03	42°53'55.40"N, 13°15'31.30"E
12	1,5E-03	42°53'55.40"N, 13°15'31.30"E
13	6,8E-02	42°53'55.40"N, 13°15'31.30"E
14	6,6E-02	42°53'55.40"N, 13°15'31.30"E
15	1,8E-03	42°53'55.40"N, 13°15'31.30"E
16	2,0E-03	42°53'55.40"N, 13°15'31.30"E
17	1,1E-02	42°53'55.40"N, 13°15'31.30"E
18	3,3E-04	42°53'55.40"N, 13°15'31.30"E
19	3,5E-01	42°53'55.40"N, 13°15'31.30"E

Table S2: K-Ar data for the gouge samples of the Sibillini Mts. Thrust

		K			⁴⁰Ar*				Age and standard deviation	
Sample ID	Grain-size fraction (µm)	Mass mg	wt %	σ (%)	Mass mg	mol/g	σ (%)	⁴⁰Ar* %	Age (Ma)	σ (Ma)
GI11	<0.1	51.2	4.949	1.4	6.568	5.593E-10	0.24	40.4	64.0	0.9
GI11	0.1-0.4	50.4	4.821	1.4	2.286	7.674E-10	0.29	55.0	89.5	1.2
GI11	0.4-2	51.1	4.286	1.4	2.674	9.680E-10	0.27	72.0	125.8	1.7
GI11	2-6	51.6	3.386	1.4	2.520	1.019E-9	0.28	86.1	165.6	2.3
GI11	6-10	50.2	3.559	1.4	2.130	1.033E-9	0.30	84.5	160.0	2.2
GI12	<0.1	51.5	4.520	1.4	2.198	5.188E-10	0.32	39.9	65.0	0.9
GI12	0.1-0.4	52.5	4.415	1.4	3.088	7.150E-10	0.26	52.9	91.0	1.2
GI12	0.4-2	53.5	4.022	1.4	2.876	8.923E-10	0.27	67.9	123.6	1.7
GI12	2-6	52.1	3.407	1.4	2.998	9.702E-10	0.26	79.7	157.1	2.2
GI12	6-10	53.3	3.313	1.4	2.524	9.621E-10	0.28	80.3	160.1	2.2

REFERENCES

- Angelier, J., 1984, Tectonic analysis of fault slip data sets. *Journal of Geophysical Research: Solid Earth*, 89(B7), 5835–5848.
- Clauer, N., & Chaudhuri, S., 1995, Clays in crustal environments: Isotope tracing and dating (359 pp.). Berlin: Springer-Verlag.
- Eberl, D.D., Środoń, J., Lee, M., Nadeau, P.H., and Northrup, H.R., 1987, Sericite from the Silverton caldera, Colorado: Correlation among structure, composition, origin, and particle thickness. *American Mineralogist*, 72, 914–934.
- Eberl, D.D., 2003, User guide to RockJock—A program for determining quantitative mineralogy from X-ray diffraction data, 40 p. U.S. Geological Survey Open File Report OF 03-78.
- Filomena, C. M., Hornung, J., & Stollhofen, H., 2014, Assessing accuracy of gas-driven permeability measurements: a comparative study of diverse Hassler-cell and probe permeameter devices. *Solid Earth*, 5(1), 1–11.
- Fossen, H., Schultz, R. A., & Torabi, A., 2011, Conditions and implications for compaction band formation in the Navajo Sandstone, Utah. *Journal of Structural Geology*, 33(10), 1477–1490.
- Fuhrmann, U., Lippolt, H. J., & Hess, J. C., 1987, Examination of some proposed K-Ar standards: ^{40}Ar / ^{39}Ar analyses and conventional K/ Ar data: Chemical Geology. Isotope Geoscience section, 66(1-2), 41–51.
- Lee, J. Y., Marti, K., Severinghaus, J. P., Kawamura, K., Yoo, H. S., Lee, J. B., & Kim, J. S., 2006, A redetermination of the isotopic abundances of atmospheric Arc. *Geochimica et Cosmochimica Acta*, 70(17), 4507–4512.
- Moore, D.M., & Reynolds, R.C. Jr., 1989, X-ray Diffraction and the Identification and Analysis of Clay Minerals. Oxford University Press, New York, 332 p.
- Ramsay, J. G., & Graham, R. H., 1970, Strain variation in shear belts. *Canadian Journal of Earth Sciences*, 7(3), 786–813.
- Schumacher, E., 1975, Herstellung von 99, 9997% ^{38}Ar für die 40K/40Ar Geochronologie. *Geochronologia Chimia*, 24, 441–442.
- Środoń, J., Drits, V.A., McCarty, D.K., Hsieh, J.C.C., and Eberl, D.D., 2001, Quantitative X-ray analysis of clay-bearing rocks from random preparations. *Clays and Clay Minerals*, 49, 514–528.
- Steiger, R., & Jäger, E., 1977, Subcommission on geochronology: Convention on the use of

decay constants in geo-and cosmochronology. *Earth and Planetary Science Letters*, 36(3), 359–362.

Torabi, A., Alaei, B., & Ellingsen, T. S. S., 2018, Faults and fractures in basement rocks, their architecture, petrophysical and mechanical properties. *Journal of Structural Geology*, 117, 256-263.